Combination of ivermectin and metformin promotes autophagy in MCF-7 cells by inhibiting phosphorylation of the PI3K/AKT/mTOR pathway

HUILI FENG[1,2], LIXIN HE[2], TALHA UMAR[2], HAIPENG WANG[1], YANLING GAO[1], GONGYI CHEN[1], PANFENG SUN[1], LING YIN[1], WENBIN ZHAO[1], HUIFANG LU[1], GANZHEN DENG[2] and CHANGWEI QIU[2]

[1]School of Pet Science and Technology, Henan Vocational College of Agriculture, Zhengzhou, Henan 451450, P.R. China; [2]Department of Clinical Veterinary Medicine, College of Veterinary Medicine, Huazhong Agricultural University, Wuhan, Hubei 430070, P.R. China

Received November 19, 2025; Accepted March 27, 2026

DOI: 10.3892/or.2026.9136

Abstract. Breast cancer remains one of the leading causes of cancer-related mortality among women globally, necessitating the exploration of novel therapeutic strategies. The present study investigated the combined effects of Ivermectin (IVM) and metformin (MET) on the human mammary tumor cell line MCF-7, with a focus on their mechanisms of action. Cell Counting Kit-8 assays were employed to evaluate proliferative activity, while Transwell migration and scratch assays assessed invasive and migratory capabilities. Transcriptomic analysis identified differentially expressed genes and key signalling pathways, while flow cytometry quantified reactive oxygen species (ROS) levels. Autophagosome formation was visualized using transmission electron microscopy. Western blotting and immunofluorescence staining were employed to detect changes in the expression of key proteins. Results demonstrated that combined IVM and MET intervention significantly inhibited MCF-7 cell viability after 24 h, showing concentration-dependent reductions in proliferation, migration and invasiveness. Transcriptomic analysis revealed a significant enrichment of the PI3K/AKT/mTOR signaling pathway, accompanied by decreased expression of thrombospondin-1 (THBS1). Western blotting revealed that the combination therapy reduced phosphorylation levels of phosphorylated (p-)PI3K, p-AKT and p-mTOR. Through the use of THBS1 overexpression plasmids, the present study validated its positive regulatory role in the PI3K/AKT/mTOR pathway, demonstrating that THBS1 mediates phosphorylation within this signaling cascade. Flow cytometry analysis demonstrated that the IVM combined with MET treatment group exhibited significantly elevated intracellular ROS levels compared with the single-drug therapy group, triggering oxidative stress responses. After clearing ROS using N-acetyl-L-cysteine, the PI3K/AKT/mTOR signaling pathway was reactivated. Additionally, transmission electron microscopy revealed extensive autophagosome formation within tumor cells of the IVM-MET combination group. The results indicate that IVM-MET inhibits PI3K/AKT/mTOR pathway phosphorylation through the accumulation of ROS and the downregulation of THBS1 expression, thereby activating autophagy programs and ultimately leading to tumor cell death.

Correspondence to: Professor Changwei Qiu, Department of Clinical Veterinary Medicine, College of Veterinary Medicine, Huazhong Agricultural University, 1 Shizishan Street, Wuhan, Hubei 430070, P.R. China
E-mail: sdqiu2001@mail.hzau.edu.cn

Abbreviations: 3-MA, 3-methyladenine; CCK-8, cell counting kit-8; IVM, Ivermectin; NAC, N-Acetyl-L-cysteine; ROS, reactive oxygen species; THBS1, thrombospondin-1

Key words: ivermectin, metformin, MCF-7, thrombospondin-1, reactive oxygen species, PI3K/AKT/mTOR, autophagy

Introduction

Breast cancer, with ~2.3 million new cases and 670,000 mortalities worldwide in 2022 (1,2), remains the most prevalent malignancy among women globally, exhibits remarkable clinical diversity and molecular heterogeneity (3). This disease not only demonstrates aggressive growth patterns but also involves complex pathogenic mechanisms regulated through multiple signaling pathways, presenting considerable therapeutic challenges. Despite recent advancements in diagnostic and therapeutic technologies, chemotherapy resistance and tumor recurrence remain key factors affecting patient outcomes (4). Current chemotherapy regimens predominantly suffer from limitations such as low therapeutic index and severe side effects. Consequently, developing novel anti-tumor drugs with both high efficacy and safety has become a key research focus (5). In this context, drug repurposing, a strategy that leverages the established pharmacological properties of existing medications to explore new therapeutic applications, has emerged as a potential frontier in oncology research.

Ivermectin (IVM), a classic antiparasitic agent, has demonstrated pharmacological effects that extend beyond its

traditional use in deworming (6). A recent study has revealed its anti-tumor efficacy through multi-target regulatory mechanisms, including the modulation of multidrug resistance proteins, interference with the Akt/mTOR-WNT signalling axis and regulation of purinergic receptor systems (7-9). Notably, metformin (MET), a commonly used clinical hypoglycemic agent, has also exhibited cross-indication anticancer properties (10), showing notable tumor-suppressive effects in various malignancies such as breast cancer (11), colorectal cancer (12), glioma (13) and oral cancer (14).

Current research on combining IVM and MET remains limited (15). Although both drugs act on the PI3K/AKT/mTOR signalling pathway, they differ markedly in their molecular targets: MET primarily inhibits mitochondrial complex I to reduce the ATP/AMP ratio and regulate mTORC1 activity, while IVM modulates cell cycle progression by affecting cyclin-dependent kinases and autophagy-related proteins (16). This complementary mechanism provides a theoretical basis for synergistic antitumor effects. From a drug development perspective, the combination of IVM and MET, both clinically validated drugs, offers advantages: i) Well-defined pharmacokinetic parameters; ii) known adverse reaction profiles; iii) avoidance of toxicity risks in new drug development. This drug repurposing strategy not only shortens research and development cycles but also considerably reduces development risks. It is expected to provide a new intervention for cancer treatment (17).

In previous years, the dual role of autophagy in tumor development has garnered increasing academic attention (18). As a highly conserved mechanism for maintaining cellular homeostasis, autophagy eliminates damaged organelles and misfolded proteins through lysosomal-mediated degradation pathways, carrying out a key role in determining the fate of tumor cells. Existing evidence suggests that moderate activation of autophagy can markedly inhibit tumor cell proliferation and induce programmed cell death (19). Notably, the central metabolic and survival signaling hub, PI3K/AKT/mTOR, serves as a key molecular switch for autophagy. Inhibiting this pathway has been shown to effectively activate the autophagic cascade, thereby exerting anti-tumor effects (20). Particularly noteworthy is the discovery that platelet-derived serum protein 1 (THBS1) acts as a notable upstream regulator of the PI3K/AKT/mTOR pathway (21). Meanwhile, reactive oxygen species (ROS), serving as important intracellular second messengers, bidirectionally regulate both the activity of this pathway and autophagy levels through redox-sensitive mechanisms (22,23).

Building on these complementary molecular mechanisms, the present study proposes an innovative strategy that combines IVM with MET, synergistically targeting the PI3K/AKT/mTOR pathway to enhance autophagy induction and thereby inhibit malignant biological behaviors in breast cancer MCF-7 cells.

Materials and methods

Reagents and antibodies. The reagents used are as follows: IVM (purity ≥98%) purchased from MilliporeSigma; MET (purity ≥98%), obtained from Macklin Inc., 3-Methyladenine (3-MA; purity ≥98%; MilliporeSigma); N-acetylcysteine (NAC; Macklin Inc.), matrix adhesive (Hangzhou Lianke Meixun Biomedical Technology Co., Ltd.) and crystal violet (Biosharp Life Sciences). p62/SQSTM Rabbit Ab (cat. no. 118420-1-AP; Proteintech Group Inc.); Phospho-AKT (cat. no. WLP001; Wanleibio Co., Ltd.); THBS1 (cat. no. A75291; Nature Biosciences LtD.); β-actin (cat. no. AC038; ABclonal Biotech Co., Ltd.); LC3B (cat. no. A19665; ABclonal Biotech Co., Ltd.); Beclin1 (cat. no. A21191; ABclonal Biotech Co., Ltd.); Bcl-2 (cat. no. A19693; ABclonal Biotech Co., Ltd.); PI3 Kinase p85 (cat. no. A4992; ABclonal Biotech Co., Ltd.); Phospho-PI3KP85α (cat. no. AP0854; ABclonal Biotech Co., Ltd.); AKT (cat. no. A20779; ABclonal Biotech Co., Ltd.); mTOR (cat. no. A11345; ABclonal Biotech Co., Ltd.); Phospho-mTOR (cat. no. AP0115; ABclonal Biotech Co., Ltd.). For Western blotting and immunofluorescence, HRP-conjugated Goat Rabbit IgG (H+L) (cat. no. AS014; ABclonal Biotech Co., Ltd.) and Alexa Flour 594-Goat Anti-Rabbit IgG (AD9279; cat. no. ABbox) were used as secondary antibodies. All antibodies were stored at -20˚C in accordance with the conditions recommended in the instructions.

Cell culture. The MCF-7 human breast cancer cell line used in the present study was kindly provided by Professor Dong Zhiqiang's laboratory at Huazhong Agricultural University, Wuhan, China. The cells were cultured in high-glucose DMEM medium (Gibco; Thermo Fisher Scientific, Inc.) supplemented with 10% fetal bovine serum (BIOVISTECH PTY. LTD) and 1% penicillin-streptomycin dual antibiotic solution (MilliporeSigma) and maintained in a constant-temperature incubator at 37˚C, 5% CO_2 and 95% humidity. When the cell confluence reached 80-90%, they were passaged using 0.25% trypsin (EDTA-containing) for 1 min at 37˚C, then divided into culture flasks at a 1:3 ratio. All experiments strictly limited cell passage to ≤15 generations, with regular mycoplasma detection and morphological observation to ensure cell viability.

Cell viability determination. MCF-7 cells in the logarithmic growth phase were prepared as single-cell suspensions ($1x10^4$ cells/ml) and inoculated into 96-well culture plates (100 μl per well), with three replicates per group. After 12 h of cell adhesion (37˚C, 5% CO_2) to achieve 50% confluency, the following treatments were administered: Blank control (with PBS only), IVM monotherapy (5-45 μmol/l), MET monotherapy (5-50 mmol/l) and combined treatment (IVM + MET; aforementioned concentrations). Treatment durations were set at 12, 24 and 48 h at 37˚C in a 5% CO_2 incubator. For mechanistic studies, cells were pre-treated with 3-MA (5 mM; 2 h) or NAC (10 mM; 2 h) at 37˚C in a 5% CO_2 incubator before receiving the final drug at 24 h. After culture termination, 100 μl working solution was added per well according to the Cell Counting Kit-8 (CCK-8; Wuhan Huiyucheng Biotechnology Co., Ltd.) protocol. The mixture was incubated at 37˚C for 30 min, followed by absorbance measurement using a Bio-Rad Laboratories, Inc. microplate reader at a wavelength of 450 nm (OD value) to assess cell viability. Three independent replicates were performed throughout the experiment to ensure data reliability.

Cell invasion test. The present study employed the Transwell invasion assay to evaluate the combined effects of IVM and

MET on the invasion of MCF-7 cells. A 100 μl Matrigel matrix gel (Xi'an Zhongtuan Biotechnology Co., Ltd.) was uniformly coated on the upper chamber of Transwell chambers (8 μM pore size; Corning, Inc.). After 4 h of polymerization at 37˚C, 100 μl of cell suspension (in serum-free DMEM) containing different treatment groups (density 5x10^4 cells/ml) was inoculated into the upper chamber. By contrast, 800 μl DMEM medium with 10% fetal bovine serum served as a chemotactic inducer in the lower chamber. The cultures were incubated at 37˚C with 5% CO_2 for 24 h. Following medium removal, cells were washed with PBS, fixed with 100% methanol for 30 min at 37˚C, stained with 0.1% crystal violet for 30 min at 37˚C and membrane-penetrating cell counts were quantified by randomly selecting 5 fields under an inverted Olympus microscope (Olympus Corporation).

Assessment of cell migration ability (scratch test). The present study evaluated the combined effects of IVM and MET on MCF-7 cell migration using a scratch assay. The protocol involved seeding MCF-7 cells at 2x10^5 cells per well in 6-well plates in DMEM supplemented with 10% fetal bovine serum, incubating them at 37˚C with 5% CO_2 for 80% fusion. A 200 μl sterile pipette was used to create vertical scratch lines perpendicular to the plate surface, followed by gentle washing with PBS to remove detached cells. Four experimental groups were established: Serum-free DMEM control, 6 μM IVM monotherapy, 6 mM MET monotherapy and IVM (6 μM) + MET (6 mM) combined intervention. All groups were cultured under identical conditions for 24 h, with the progress of scratch closure monitored every 8 h using an inverted microscope (100x; Olympus CKX41; Olympus Corporation). Migration area changes were quantified using ImageJ software (version 1.53e; National Institutes of Health) to evaluate treatment effects.

Measurement of intracellular ROS. The ROS levels in MCF-7 cells were detected using the 2',7'-Dichlorodihydrofluorescein diacetate (DCFH-DA) fluorescence probe method. The experimental protocol was as follows: MCF-7 cells were seeded at 2x10^5 cells per well and cultured in 6-well plates until 70% confluency, then subjected to the following treatments: i) Different drug groups (PBS, IVM, MET and combination therapy) for 12 or 24 h at 37˚C in a 5% CO_2 incubator; ii) drug administration after 2 h pretreatment with 10 mM NAC; iii) positive control [Ros up (a compound mixture that induces ROS production); 50 μg/ml stimulation for 20 min at 37˚C; Beyotime Biotechnology]. Cells were collected and adjusted to a density of 1x10^9 cells/ml. Then, they were incubated with a 10 μM DCFH-DA probe (Wuhan Huiyucheng Biotechnology Co., Ltd.) at 37˚C in the dark for 30 min. After washing 3x with PBS and resuspension, the fluorescence intensity was measured using a flow cytometer (CytoFLEX; Beckman Coulter) with excitation/emission wavelengths of 488 nm and 530 nm, respectively. Each group had 3 duplicate wells, and the experiment was independently repeated 3 times. Data were expressed as mean fluorescence intensity ± SD.

Transmission electron microscopy observation. The present study employed a transmission electron microscope (accelerated voltage 100 kV; Hitachi H7650; Hitachi, Ltd.) to investigate the effects of IVM, MET and their combination on the ultrastructure of MCF-7 cells. Cells were inoculated into 6-well plates (1x10^5 cells per well). After achieving 60-70% fusion, they were treated with the respective drugs (PBS, IVM, MET or IVM + MET) for 24 h at 37˚C in a 5% CO_2 incubator. After fixation with 2.5% glutaraldehyde for 2 h at 4˚C, the samples underwent an ethanol gradient dehydration process (50, 70, 90 and 100%) followed by epoxy resin embedding and polymerization at 60˚C for 48 h and ultra-thin sectioning (80 nm, using a Leica UC6 microtome; Leica Microsystems). Uranium acetate staining for 30 min at room temperature in the dark was applied to enhance contrast. A total of 10 random fields from each group were systematically observed, with a particular focus on analyzing autophagosome formation and morphological changes in organelles, such as mitochondria and the endoplasmic reticulum.

Western blotting. The present study systematically evaluated the effects of various treatment protocols on protein expression profiles in MCF-7 cells using western blot analysis. The experimental protocol was as follows: MCF-7 cells were cultured in 6-well plates until 80% confluency, after which the following groups were established: i) PBS control group, IVM single drug group (6 μM), MET single drug group (6 mM) and combined treatment group, all treated for 24 h at 37˚C in a 5% CO_2 incubator; ii) Autophagy inhibitor pretreatment group (5mM 3-MA administered 2 h prior to treatment at 37˚C in a 5% CO_2 incubator). Experimental procedures included collecting cells, washing them 3 times with pre-chilled PBS, adding RIPA lysis buffer (containing protease inhibitors; cat. no. P0013B; Beyotime Biotechnology) for lysing on ice for 30 min. Protein concentrations were measured using the BCA Protein Quantification Kit (Thermo Fisher Scientific Inc.) and adjusted to a uniform concentration of 15 μg/well. Protein samples were separated by 10% SDS-PAGE and transferred to a PVDF membrane using the gel-membrane sandwich that was submerged in transfer buffer and electrophoresed at constant voltage. Subsequent steps included blocking (5% skim milk; room temperature for 2 h), primary antibody incubation at 4˚C overnight with the following dilutions: p62/SQSTM (1:1,000), Phospho-AKT (1:500), THBS1 (1:500), β-actin (1:2,000), LC3B (1:1,000), Beclin1 (1:1,000), Bcl-2 (1:1,000), PI3K p85 (1:1,000), Phospho-PI3K p85 (1:500), AKT (1:1,000), mTOR (1:1,000) and Phospho-mTOR (1:500) secondary antibody incubation (HRP-labelled; 1:5,000 dilution; room temperature for 2 h). Finally, signals were detected using a Fusion FX7 chemiluminescence imaging system and quantified with ImageJ software (version 1.53e; National Institutes of Health) to analyze the expression ratio of the target protein to the internal control β-actin. To ensure experimental reliability, all experiments included three independent biological replicates.

Construction of overexpressed plasmids. The present study employed molecular cloning techniques to construct an overexpression vector for the THBS1 gene. Specific primers based on the mouse THBS1 coding sequence (accession no. NP_035710.2) from the GenBank database (https://www.ncbi.nlm.nih.gov/genbank/) were first designed to amplify the target gene. The primer sequences used for amplifying the mouse THBS1 CDS were as follows: Forward, 5'-CTATAG

GGAGACCCAAGCTGGCTAGCGCCACCATGGAGCTCC TGCGGGGACTAGGTGTCCTGTTCCTGTTGCATATG-3'; reverse, 5'-GTTTAAACGGGCCCTCTAGACTCGAGT TAAGCGTAGTCTGGGACGTCGTATGGGTAGGAATCT CGACACTCGTATTTC-3'. The reverse primer sequence is presented in its full-length synthesized form, which includes a 5' vector homology arm (for In-Fusion cloning) and a sequence encoding a C-terminal HA tag (Tyr-Pro-Tyr-Asp-Val-Pro-Asp-Tyr-Ala) immediately upstream of the THBS1 gene-specific region. For sequence verification purposes, only the gene-specific portion should be used for BLAST alignment against the mouse THBS1 reference sequence. Using MCF-7 cell cDNA as a template, PCR amplification was performed with PrimeSTAR HS high-fidelity DNA polymerase (Takara Bio, Inc.) to ensure genetic accuracy. The amplified products were digested with NheI/XhoI restriction endonucleases (Thermo Fisher Scientific, Inc.) and ligated to the homologous pcDNA3.1 (+) eukaryotic expression vector. The recombinant plasmid was transformed into DH5α competent cells (Beijing Quanshijin Biotechnology Co., Ltd.) via the heat shock method, followed by ampicillin resistance screening to identify positive clones. After Sanger sequencing (Shenzhen BGI Genomics Co., Ltd.) confirmed the correct insertion sequences, the vector (2 μg per well of a 6-well plate) was introduced into MCF-7 cells using Lipofectamine® 3000 (Invitrogen; Thermo Fisher Scientific, Inc.) via liposome transfection at 37˚C in a 5% CO_2 incubator for 6 h, after which the medium was replaced with fresh complete medium. Western blotting was used to verify the expression levels of THBS1 protein. In these experiments, cells transfected with the empty pcDNA3.1(+) vector served as the negative control.

Immunofluorescence experiment. The present study utilized immunofluorescence technology to assess the effects of various treatments on MCF-7 cells. MCF-7 cells were cultured at a density of $1x10^4$ cells per well in 24-well plates until they reached 80% confluency. A total of four treatment groups were established: Blank control (PBS), 6 μM IVM (IVM monotherapy), 6 mM MET (MET monotherapy) and combined treatment group (6 μM IVM + 6 mM MET). After 24-h treatment, cells were washed with PBS, fixed in 4% polyformaldehyde (Biosharp Life Sciences) for 30 min at room temperature, permeabilized with 0.2% Triton X-100 for 15 min at room temperature and blocked with 5% goat serum for 2 h at room temperature. Samples were incubated with specific primary antibodies at the following dilutions: Anti-LC3B (1:200) and anti-p62 (1:200) overnight at 4˚C, followed by a 2-h incubation at room temperature in the dark with a FITC-labelled secondary antibody (1:500). DAPI staining (Biosharp Life Sciences) was performed for 5 min at room temperature. The cells were observed under a fluorescence microscope (Olympus IX73; Olympus Corporation).

Statistical analysis. This study employed standardized statistical methods to process and analyze the experimental data. All quantitative data were derived from three independent biological replicate experiments, presented as mean ± SD. Data analysis was conducted using GraphPad Prism 10.1 (Dotmatics) professional statistical software, with one-way ANOVA primarily used for intergroup comparisons, supplemented by Tukey's post hoc tests for multiple comparisons. Statistical significance thresholds were defined as follows: $P<0.05$ indicates a statistically significant difference, $P<0.01$ denotes highly significant differences, $P<0.001$ signifies extremely significant differences, while $P>0.05$ (marked as ns) indicates no statistically significant difference.

Results

IVM combined with MET inhibits the proliferative activity of MCF-7 cells in vitro. Results of the present study demonstrated that both IVM and MET monotherapy reduced MCF-7 cell viability, exhibiting typical concentration-dependent and time-dependent characteristics (Fig. 1A and B). Through the calculation of half-inhibitory concentrations (I) and orthogonal experimental analysis, the optimal combination concentration was determined to be 6 μM IVM combined with 6 mM MET, which confirmed the enhanced inhibitory effect of the combination (Fig. 1C). Notably, the combined treatment group exhibited a significant synergistic effect, demonstrating markedly improved inhibitory efficacy when compared with either monotherapy (Fig. 1D). This optimized formulation was subsequently employed in subsequent experimental studies.

IVM combined with MET inhibits the invasion and migration of MCF-7 cells in vitro. The combination of IVM and MET demonstrated significant inhibitory effects on the malignant phenotype of MCF-7 cells. Transwell invasion assays revealed that, compared with the control group and single-drug treatment groups, the combined treatment group exhibited a markedly reduced cell invasion capacity (Fig. 2A and B). The scratch-healing assay further indicated that the drug-coated treatment group exhibited significantly slower cell migration rates compared with both the control and single-drug treatment groups (Fig. 2C and D). These data collectively demonstrate that the synergistic application of IVM and MET effectively suppresses the invasive migration capabilities of breast cancer cells.

IVM combined with MET decreases the expression level of THBS1 protein. During the development of breast tumors, various cytokines and protein molecules carry out key roles. THBS1, a key extracellular matrix protein, is associated with tumor cell proliferation, migration and invasion (24). Western blot analysis revealed that, compared with the control group and single-drug treatment groups, the IVM combined with MET treatment significantly reduced THBS1 expression in MCF-7 cells, with statistically significant difference; (Fig. 3A and B). These results demonstrate that the IVM combined with MET effectively suppresses THBS1 expression in breast cancer cells.

IVM combined with MET reduced the phosphorylation level of the PI3K/AKT/mTOR pathway. The PI3K/AKT/mTOR signaling pathway plays a key role in the development of tumors (25). The present study employed western blotting to evaluate the effects of different drug combinations on phosphorylation levels within this pathway. Results demonstrated that when IVM was combined with MET treatment, intracellular phosphorylation levels of phosphorylated (p)-PI3K,

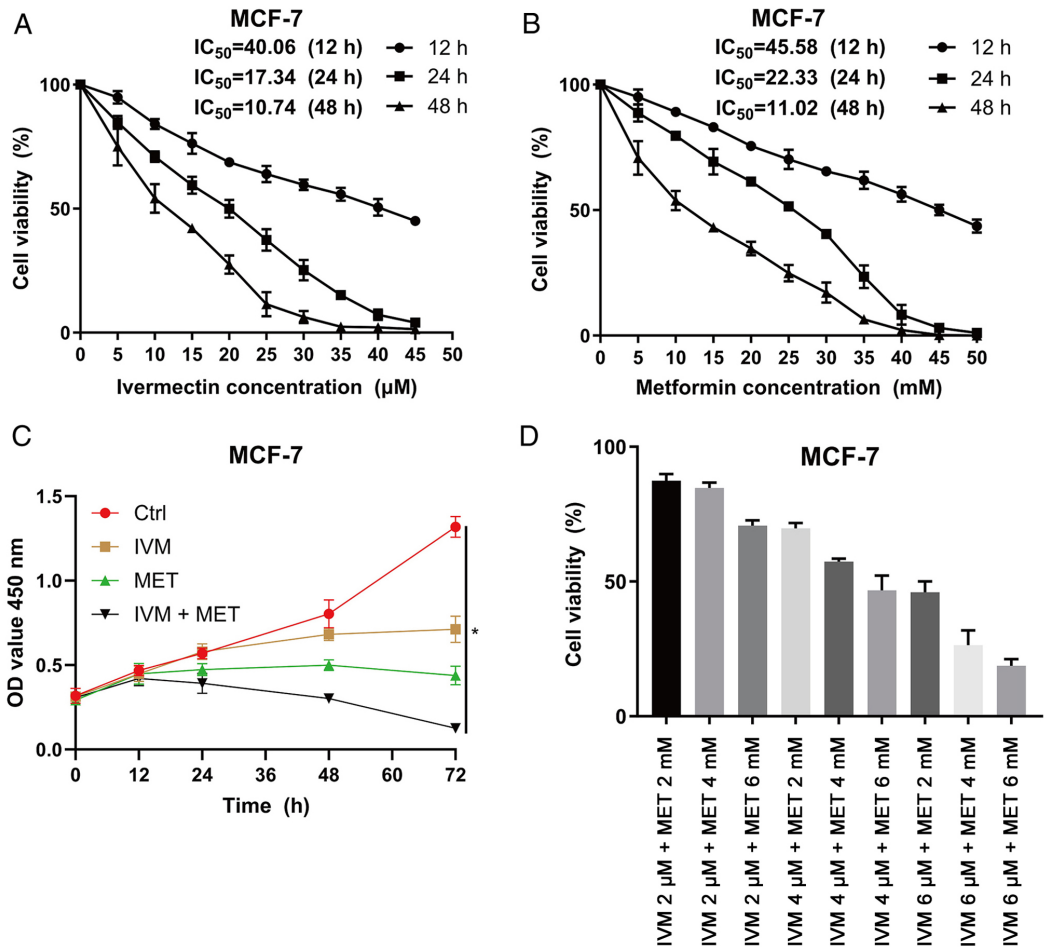

Figure 1. Effects of IVM, MET and the combination of the two drugs on the toxicity and proliferation of MCF-7 cells. (A) Cell viability assays after treatment of MCF-7 cells with IVM. (B) Cell viability assays after treatment of MCF-7 cells with MET. (C) CCK-8 assay evaluating cell viability in MCF-7 cells treated with PBS, IVM, MET and IVM + MET at 0, 12, 24, 48 and 72 h; (D) Comparison of MCF-7 cell viability after co-treatment with 2, 4 μM and 6 mMdoses of IVM combined with 2, 4 and 6 mmol/l doses of MET using the CCK-8 method. CCK-8, Cell Counting Kit-8; IVM, ivermectin; MET, metformin, MCF-7, human mammary tumor cell line; Ctrl, control. All data were measured as mean ± SEM by three independent experiments. *P<0.05.

p-AKT and p-mTOR were significantly reduced in MCF-7 cells compared with control groups and single-drug treatments (Fig. 4A and B). These findings suggest that the IVM-MET combination may target the PI3K/AKT/mTOR pathway and induce tumor cell death.

Overexpression of THBS1 enhances the levels of phosphorylated PI3K, AKT and mTOR. Studies have demonstrated that the expression of THBS1 is regulated by the PI3K/AKT/mTOR signaling pathway (21,26). To investigate whether THBS1 exerts feedback regulation on this pathway, the present study utilized transcriptome data (NP_035710.2; NCBI database). The present study identified the CDS region of THBS1 from the National Centre for Biotechnology Information (NCBI) database. Using pcDNA3.1 (+) as the vector, an overexpression plasmid for THBS1 was constructed (Fig. 5A). Agarose gel electrophoresis revealed amplified gene fragments from the THBS1 CDS region, measuring 3558 bp in length (Fig. 5B).

The THBS1 overexpression construct used in this study was originally generated for parallel investigations in mouse and canine mammary tumor models, leveraging the high cross-species conservation of THBS1. Its application in human MCF-7 cells is supported by the >97% amino acid sequence identity between mouse and human THBS1, ensuring functional relevance (27).

Western blotting was used to detect the overexpression efficiency of THBS1 in MCF-7 cells, transfected with the empty pcDNA3.1(+) vector serving as the negative control. The results showed that, compared with the Ctrl group and the negative control [pcDNA3.1(+)] group, the overexpression efficiency of THBS1 was significantly increased (Fig. 5C and D).

IVM combined with MET induces autophagy in MCF-7 cells. Disruption of autophagy is associated with the development and progression of various diseases. To investigate the effects of IVM combined with MET on autophagy in breast tumors, the present study employed cellular immunofluorescence to detect autophagy-related proteins LC3B and p62 in MCF-7 cells. The results showed that compared with the control group, the combined treatment group exhibited elevated LC3B expression (Fig. 6A) and decreased p62 levels (Fig. 6B), indicating that IVM combined with MET can induce excessive autophagy in breast tumor cells. Excessive autophagy leads to over-degradation of multiple cellular components. Transmission electron microscopy analysis revealed that, compared with the control group and single-drug treatment groups, the IVM + MET

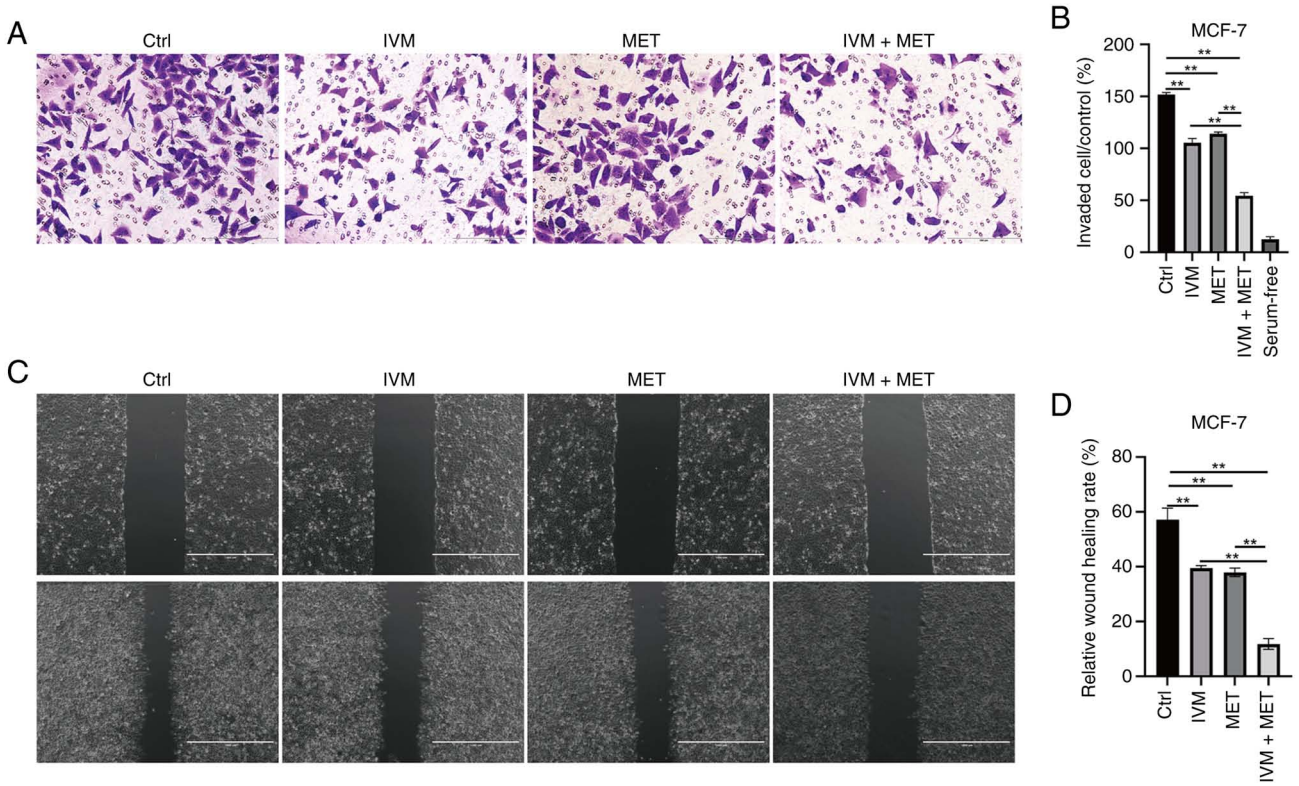

Figure 2. IVM combined with MET inhibits the invasive and migratory ability of MCF-7 cells. (A) Representative Transwell images and (B) quantification of the invasive ability of MCF-7 cells. (C) Representative scratch images and (D) quantification of the migration ability in [Ctrl, IVM (6 μM), MET (6 mM), and IVM + MET] groups of MCF-7 cells. IVM, ivermectin; MET, metformin, MCF-7, human mammary tumor cell line; Ctrl, control. All data were measured as mean ± SEM by three independent experiments. **P<0.01.

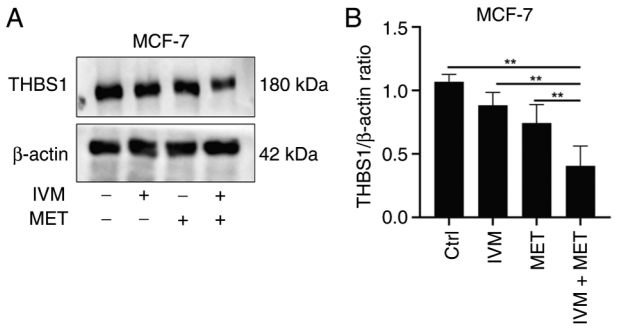

Figure 3. Western blotting detection of THBS1 protein expression in MCF-7 cells. (A) Representative western blotting image shows the expression of THBS1 protein in MCF-7 cells was downregulated. The molecular weights of THBS1 and β-actin are indicated as 180 and 42 kDa, respectively. (B) Semi-quantification of the western blotting results. IVM, ivermectin (6 μM); MET, metformin (6 mM); MCF-7, human mammary tumor cell line; Ctrl, control; +, with treatment. All data were measured as mean ± SEM by three independent experiments. **P<0.01.

group contained numerous double-membrane-structured autophagosomes and an increased number of autophagic lysosomes (Fig. 6C). Western blot analysis revealed that, compared with the PBS control group, LC3B and Beclin1 protein expressions were upregulated in MCF-7 cells after IVM, MET and IVM + MET treatments, while p62 and Bcl2 were downregulated (Fig. 6D and E). These results demonstrate that IVM, when combined with MET, can promote autophagy in MCF-7 cells.3-MA is an early-stage autophagy inhibitor (28). To investigate how autophagy inhibition affects cytotoxicity caused by IVM combined with MET, the present used the CCK-8 assay to evaluate the effects of co-treatment with 3-MA and/or IVM + MET on cell viability. The results showed that the co-treated group exhibited a significant rebound in cell activity compared with the IVM + MET-only group (Fig. 6F).

IVM combined with MET promotes autophagy of breast tumor cells through ROS. Flow cytometry analysis of ROS in MCF-7 cells revealed significantly elevated intracellular ROS levels following IVM and MET treatments compared with the control group, with the combined IVM + MET treatment showing even higher ROS levels (P<0.05; Fig. 7A and B). This suggests that the IVM + MET regimen may induce oxidative stress by increasing intracellular ROS, thereby affecting cell survival and function. NAC, an antioxidant that reduces intracellular ROS (29).

MCF-7 cells were pre-treated with 10 mM NAC in the present study (NAC group). Subsequent experimental groups included Ctrl, IVM + MET and IVM + MET + NAC. After 24 h of stimulation, ROS levels were measured using flow cytometry. Results demonstrated a partial reduction in ROS levels in the IVM + MET + NAC group compared with the IVM + MET group (Fig. 7C and D). To investigate whether IVM + MET affects PI3K/AKT/mTOR pathway phosphorylation through ROS, western blotting was employed to detect p-PI3K, p-AKT and p-mTOR protein expression in MCF-7 cells. The results demonstrated that IVM + MET inhibited phosphorylation activity in the PI3K/AKT/mTOR signaling

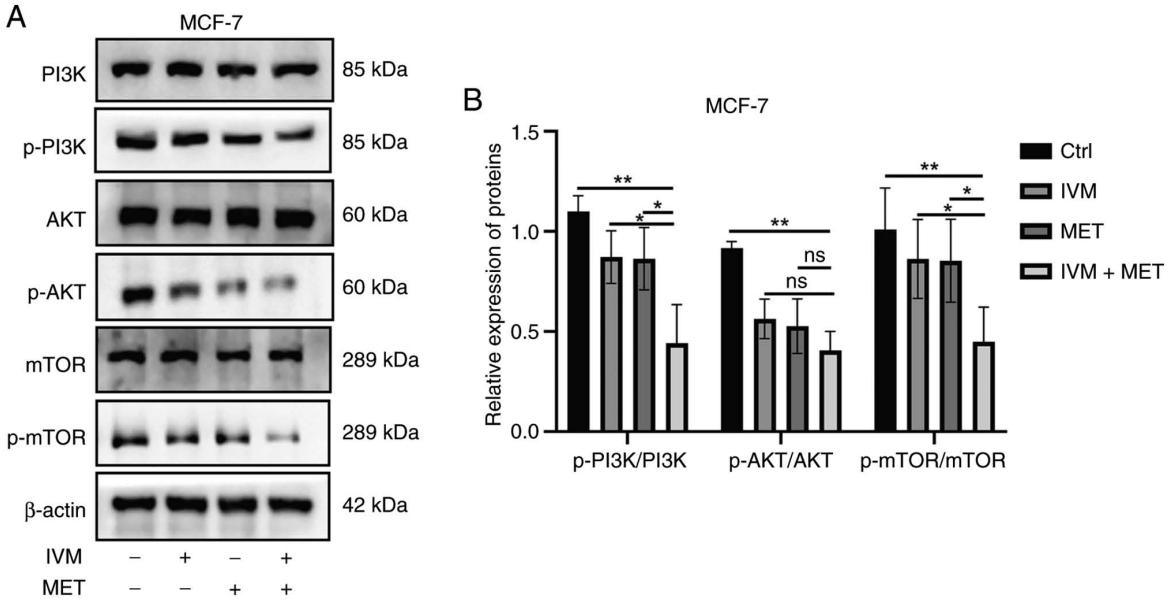

Figure 4. IVM combined with MET reduces the phosphorylation levels of proteins in the PI3K/AKT/mTOR pathway. (A) Representative images of western blotting and, (B) The expression levels of PI3K, AKT, mTOR and their phosphorylated proteins in MCF-7 cells treated with PBS, IVM, and IVM + MET. IVM, ivermectin; MET, metformin, MCF-7, human mammary tumor cell line; Ctrl, control; p, phosphorylated. All data were measured as mean ± SEM by three independent experiments. *P<0.05, **P<0.01.

pathway compared with Ctrl and single-drug treatments, and this inhibition was associated with elevated intracellular ROS levels. Furthermore, compared with the IVM + MET group, the IVM + MET + NAC group showed a partial elevation in protein expression levels of p-PI3K, p-AKT and p-mTOR (Fig. 7E and F). This suggests that the combination of IVM and MET may suppress phosphorylation levels in the PI3K/AKT/mTOR signaling pathway by inducing ROS accumulation. When intracellular ROS levels increase, key proteins in the PI3K/AKT/mTOR signaling pathway undergo oxidative modifications, resulting in reduced activity (30). To investigate whether the IVM + MET combination could alter autophagy-related proteins via ROS, western blot analysis was performed on MCF-7 cells for LC3B, Beclin1, p62 and Bcl-2. Results revealed that, compared with the IVM + MET group, the IVM + MET + NAC group exhibited partial decreases in LC3B and Beclin1 protein expression, while showing partial increases in p62 and Bcl-2 expression (Fig. 7G and H). These findings suggest that the IVM + MET combination inhibits the phosphorylation of the PI3K/AKT/mTOR signaling pathway by inducing excessive ROS accumulation within cells, thereby triggering tumor cell autophagy and exerting antitumor effects.

Discussion

Biosynthetic inhibition (IVM) combined with meta protection (MET) demonstrated potent antitumor effects on MCF-7 breast cancer cells, effectively suppressing their proliferation, migration and invasiveness. These findings suggest that the combined therapy may exert its anti-tumor efficacy by modulating key biological processes in tumor cells. RNA sequencing has emerged as a powerful and versatile tool for gene expression analysis (31). Transcriptomic analysis of drug combinations in mouse models from NCBI revealed 53 differentially expressed genes across the PBS-treated control (Ctrl), IVM (6 μM) + Ctrl, MET (6 mM) + Ctrl, and IVM (6 μM) + MET (6 mM) groups. The grouping strategy included comparisons of the combination treatment against the Ctrl, as well as against each single agent (IVM or MET alone), as shown in the experimental design.

IVM + PBS-treated control (Ctrl), MET + Ctrl and IVM + MET groups. GO enrichment analysis identified key functional pathways, including protein trafficking, cell differentiation, DNA repair, signaling pathways and ubiquitination. KEGG pathway analysis revealed considerable enrichment in PI3K/AKT/mTOR, MAPK signaling and tumor-related pathways. Our transcriptional studies further demonstrate that IVM and MET synergistically regulate THBS1. As THBS1 is associated with activation of the PI3K/AKT/mTOR pathway, overexpression of THBS1 enhances PI3K/AKT phosphorylation, thereby promoting glioma cell migration and proliferation (32,33). Conversely, THBS1 knockdown inhibits activation of the PI3K/AKT signaling pathway (34). In the present study, the combination of IVM and MET reduced the protein expression level of THBS1 and inhibited the activation of the PI3K/AKT/mTOR signaling pathway. To further validate these findings, the THBS1-pCDNA3.1(+) vector was transfected into MCF-7 cells to achieve overexpression of THBS1 protein. Experimental results demonstrated that the overexpression of THBS1 partially restored phosphorylation levels in this signaling pathway. These findings suggest that the combination of IVM and MET may target THBS1 to inhibit tumor cell proliferation and survival, indicating a novel approach for developing anti-tumor drugs that target the PI3K/AKT/mTOR signaling pathway. however, further *in vitro* and *in vivo* experiments would first be required.

PI3K/AKT/mTOR is highly associated with autophagy. Studies have shown that hawthorn acid can inhibit the protein expression of PI3K-p110α, p-Akt and p-mTOR, thereby inducing autophagy in nasopharyngeal carcinoma cells (35,36). Glycyrrhizin A can suppress the phosphorylation of the PI3K/AKT/mTOR signaling pathway, promoting

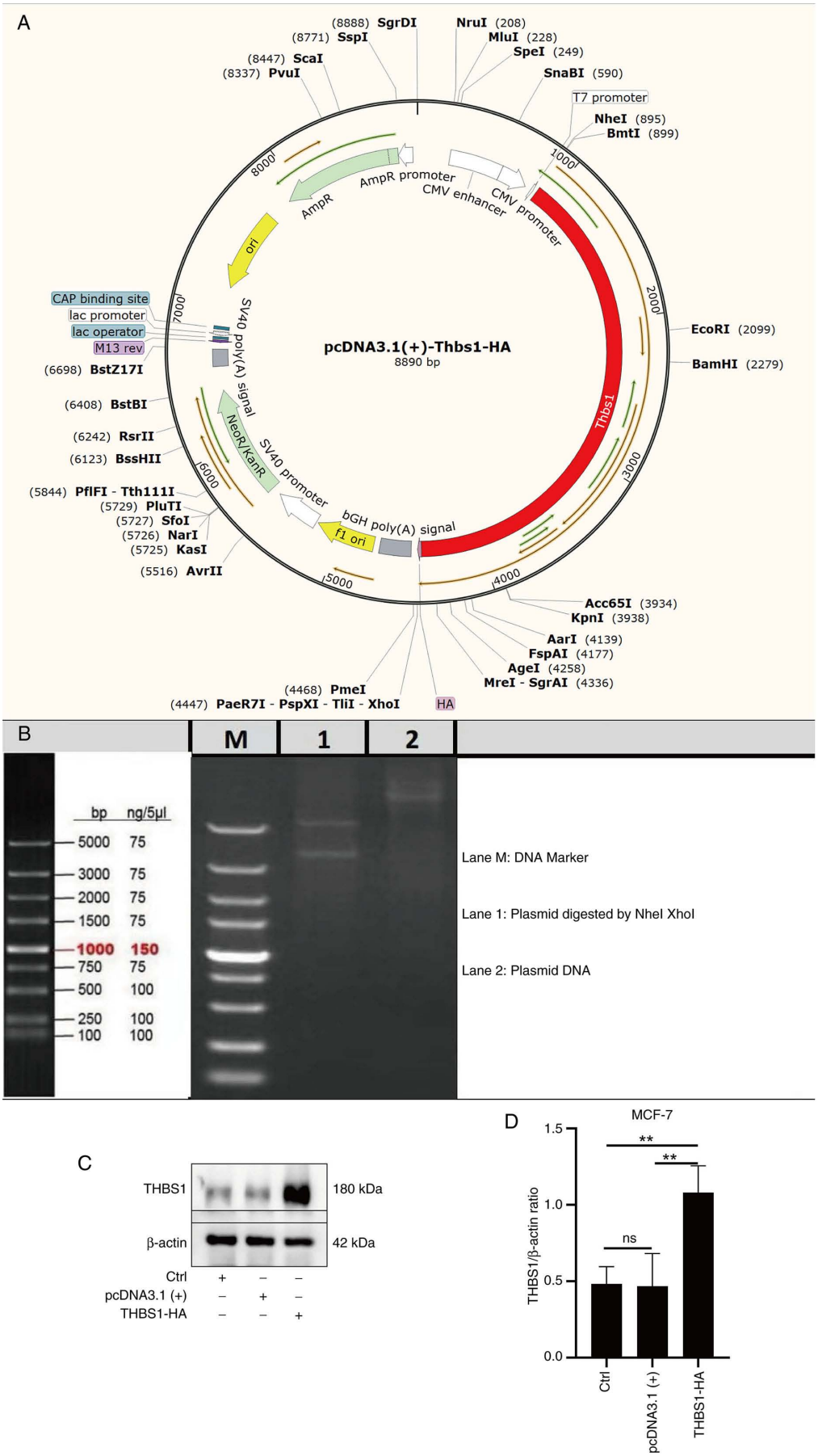

Figure 5. Overexpression of THBS1 enhances the phosphorylation level of proteins in the PI3K/AKT/mTOR pathway. (A) Schematic diagram of THBS1 overexpression plasmid construction. (B) Detection of THBS1 CDS region amplification by agarose gel electrophoresis. (C) Representative western blotting images and (D) semi-quantification of THBS1 overexpression efficiency in MCF-7 cells. MCF-7, human mammary tumor cell line. All data were measured as mean ± SEM by three independent experiments. $^{**}P<0.01$.

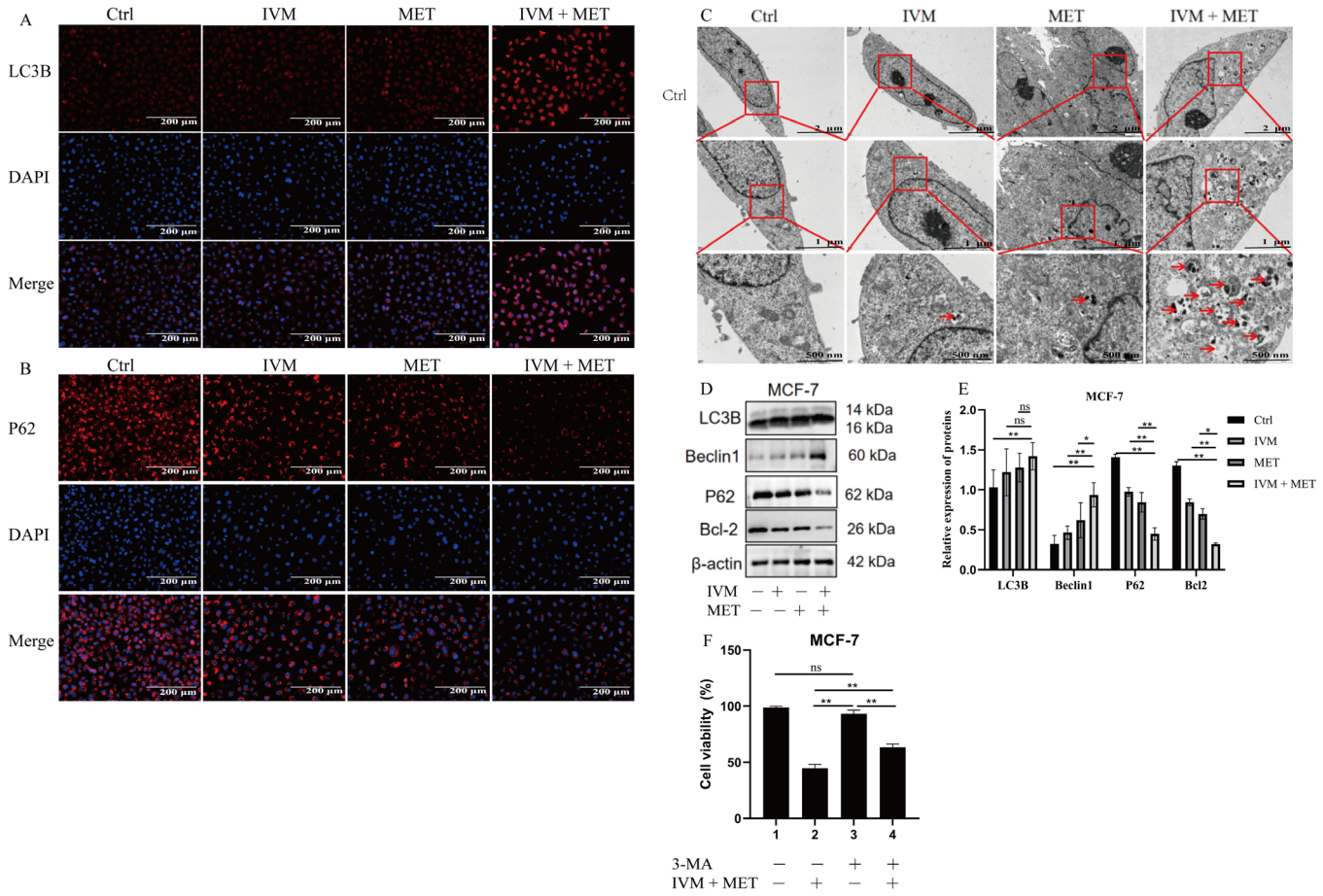

Figure 6. Autophagy induction in MCF-7 cells by IVM combined with MET. (A) Representative immunofluorescence images showing the expression and localization of the autophagosome marker LC3B (red) in MCF-7 cells treated with PBS (Ctrl), IVM (6 μM), MET (6 mM) or IVM + MET for 24 h. Nuclei are stained with DAPI (blue). The pronounced increase in LC3B puncta formation (indicated by arrows) in the IVM + MET-treated group indicates autophagosome accumulation, a hallmark of autophagy induction. Scale bar, 200 μm. (B) Representative immunofluorescence images showing the expression and localization of the autophagic flux marker p62/SQSTM1 (red) in MCF-7 cells under the same treatment conditions as in (A). Nuclei are stained with DAPI (blue). The marked reduction in p62 fluorescence intensity in the IVM + MET-treated group reflects enhanced autophagic degradation, confirming active autophagic flux. Scale bar, 200 μm. (C) Representative transmission electron microscopy images of MCF-7 cells following 24 h of treatment. Images are shown at increasing magnifications with scale bars of 2 μm (top), 1 μm (middle), and 500 nm (bottom) for each treatment group (Ctrl, IVM, MET and IVM + MET). Numerous double-membrane autophagosomes (indicated by red arrows) are evident in the IVM + MET-treated cells, providing ultrastructural confirmation of autophagy activation. (D) Western blot analysis of key autophagy-related proteins (LC3B-I/II, Beclin1, p62 and Bcl-2) in MCF-7 cells treated as indicated for 24 h. β-actin serves as the loading control. (E) Densitometric semi-quantification of the protein levels. (F) Cell viability assessment by Cell Counting Kit-8 assay. Pre-treatment with 3-MA significantly rescued the loss of cell viability induced by IVM + MET, confirming the functional contribution of autophagy to the cytotoxic effect. IVM, ivermectin; MET, metformin, MCF-7, human mammary tumor cell line; Ctrl, control. All data were measured as mean ± SEM by three independent experiments. *P<0.05, **P<0.01.

autophagy in renal cancer cells (37). Berberine II inhibits the PI3K/AKT/mTOR pathway, enhancing autophagy in MCF-7 cells (38). Therefore, the present study investigated the PI3K/AKT/mTOR pathway to elucidate the molecular mechanisms underlying the interaction between IVM and MET, as well as the role of autophagy. Western blotting results revealed that IVM combined with MET inhibited the phosphorylation in the PI3K/AKT/mTOR pathway, consistent with findings from another tumor study (39). Immunofluorescence analysis of LC3B and p62 proteins in MCF-7 cells revealed increased LC3B levels and decreased p62 levels. Transmission electron microscopy observations of autophagosome formation in Ctrl, IVM, MET and IVM + MET groups demonstrated that the IVM + MET group had the highest volume of autophagosomes. Western blot analysis of LC3B and p62 expression in all three cell types revealed that IVM, combined with MET, upregulated LC3B expression while downregulating p62.

Based on these findings, the present study concluded that the combination of IVM and MET inhibits the phosphorylation of protein in the PI3K/AKT/mTOR pathway, thereby promoting excessive autophagy in tumor cells. The present study revealed that both the activation level of the PI3K/AKT/mTOR pathway and autophagy levels can be regulated by ROS. The effects of IVM combined with MET on ROS levels in breast tumor cells using *in vitro* experiments were first examined. Results revealed that, compared with using either IVM or MET alone, the ROS levels in breast tumor cells were increased under the combined treatment group. This suggests that the synergistic effect of IVM and MET may stem from their ability to elevate intracellular ROS levels. ROS, as products of oxidative stress within cells, exhibit diverse biological functions. Under normal physiological conditions, intracellular ROS levels remain relatively stable. However, in tumor cells, disrupted redox balance often leads to elevated ROS concentrations (40). Previous research has

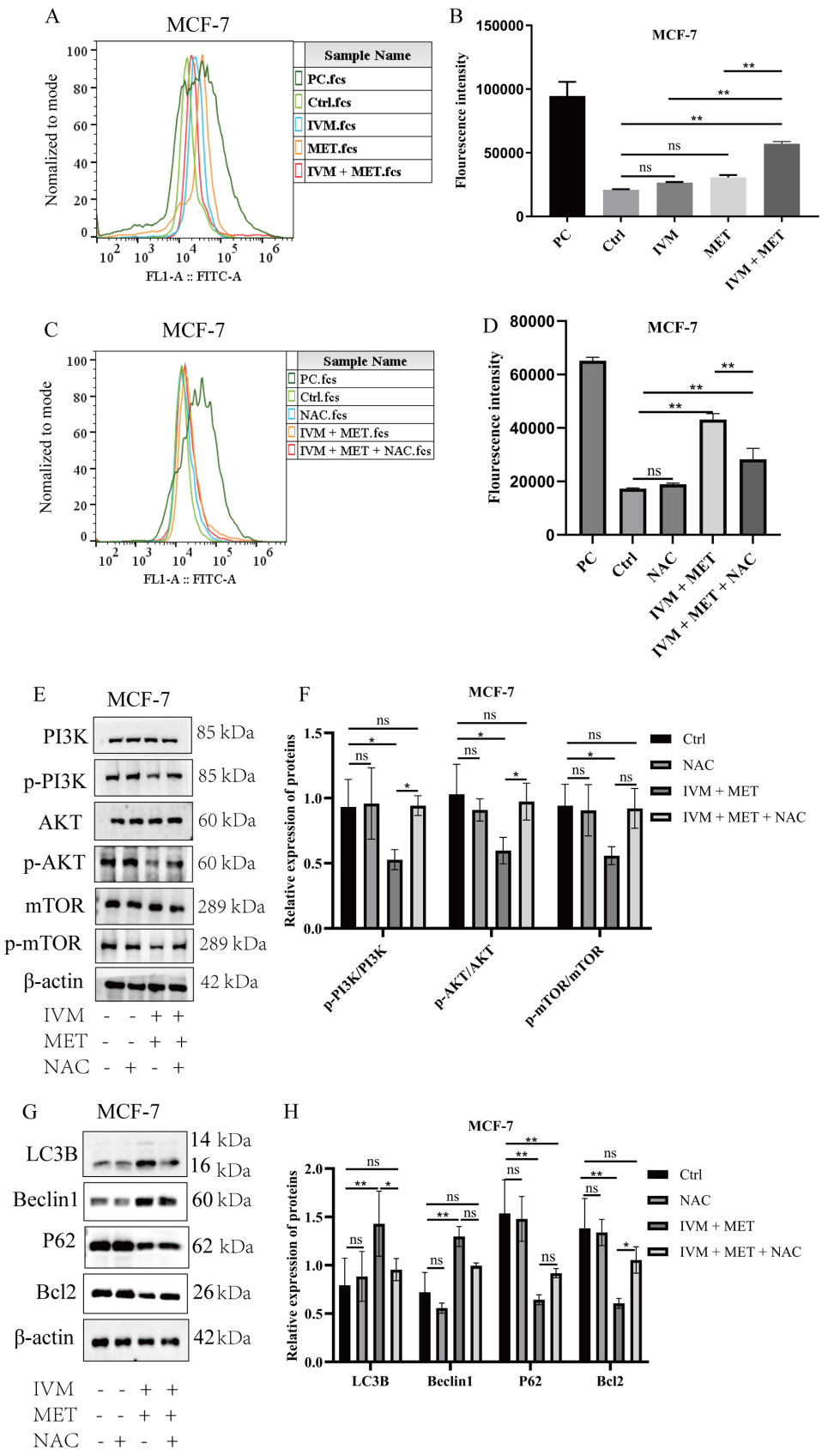

Figure 7. IVM combined with MET promotes the accumulation of ROS in MCF-7 cells. (A) Representative flow cytometry plot and (B) quantification of ROS expression levels in MCF-7 cells after treatment with different experimental groups. PC, Ctrl, IVM, MET and IVM + MET groups are shown. (C) Representative flow cytometry plot and (D) quantification of ROS expression levels in MCF-7 cells after treatment with NAC. PC, Ctrl, IVM, MET, and IVM + MET groups are shown. (E) Representative western blotting images and (F) semi-quantification of p-PI3K, p-AKT and p-mTOR protein expression levels in MCF-7 cells after treatment with different experimental groups; (G) Representative western blotting images and (H) semi-quantification of autophagy-related protein expression levels in MCF-7 cells treated with PBS, IVM, MET and IVM + MET. ROS, reactive oxygen species; p, phosphorylated; IVM, ivermectin; MET, metformin, MCF-7, human mammary tumor cell line; Ctrl, control; PC, positive control. All data were measured as mean ± SEM by three independent experiments. *P<0.05, **P<0.01.

demonstrated that star fruit root can inhibit cardiomyocyte apoptosis by regulating ROS-mediated PI3K/AKT/mTOR autophagy pathways (41). Findings of the present study indicated that IVM combined with MET induces excessive ROS accumulation and further promotes autophagy in breast tumor cells, suggesting that ROS regulation may constitute another key mechanism by which IVM and MET suppress tumor biology.

Autophagy, a process that involves the degradation and recycling of intracellular material, can inhibit tumor development during its early stages (42). The accumulation of ROS can induce cellular oxidative stress, impairing cell proliferation and survival by triggering autophagy. To investigate their interplay, pre-treatment with NAC (a ROS scavenger) was employed. Results demonstrated that NAC alleviates ROS overproduction caused by the combination of IVM and MET, partially restores phosphorylation levels in the PI3K/AKT/mTOR signaling pathway and reduces autophagy in breast cancer cells. However, the present study has limitations. First, the *in vitro* model, while controlled, does not fully recapitulate the complex tumor microenvironment *in vivo*. Second, while NAC was used to establish the functional role of ROS, future investigations could characterize the specific alterations in the antioxidant defense system (for example, superoxide dismutase, catalase or glutathione peroxidase activity) in response to IVM + MET treatment to fully delineate the redox adaptations involved. Another limitation of the present study is the lack of a pharmacological positive control (for example rapamycin) in the immunofluorescence assay for autophagy. However, the conclusion of the present study is supported by the convergence of evidence from transmission electron microscopy (direct observation of autophagosomes), western blot analysis of autophagic flux markers and a functional rescue experiment using the autophagy inhibitor 3-MA. These findings suggest that the synergistic effect of IVM and MET may stem from the elevation of ROS, subsequent suppression of the PI3K/AKT/mTOR pathway phosphorylation and induction of autophagy. This discovery provides a scientific foundation for exploring the therapeutic applications of IVM and MET in the treatment of breast cancer.

Acknowledgements

Not applicable.

Funding

The present study was supported by a research grant 'Dandelion Sterol Inhibits the Proliferation and Migration of Human and Canine Breast Tumor Cells' (grant no. 2505NDLX06), Henan Vocational College of Agriculture, 2025.5. 'Clinical Diagnosis and Prevention Techniques for Canine Breast Tumor in Veterinary Medicine' (grant no. 2505RCLX02), Henan Vocational College of Agricultural, 2025.5. 'Innovative Research Team in Pet Medical Technology' (grant no. 2505TDLX05), Henan Vocational College of Agricultural, 2025.5.

Availability of data and materials

The data generated in the present study may be requested from the corresponding author.

Authors' contributions

HF and CQ contributed to conceptualization; HF, LH and TU contributed to methodology; HW, LY and GC contributed to data analysis; PS, WZ and HL contributed to formal analysis; CQ contributed to resources, investigation, supervision, project administration, data curation, validation and funding acquisition; GD contributed to data curation, visualization and validation; HF contributed to writing of the original draft and TU contributed to reviewing and editing. HF and CQ confirm the authenticity of data. All authors have read and agreed to the published version of the manuscript.

Ethics approval and consent to participate

Not applicable.

Patient consent for publication

Not applicable.

Competing interests

The authors declare that they have no competing interests.

References

1. Kim J, Harper A, McCormack V, Sung H, Houssami N, Morgan E, Mutebi M, Garvey G, Soerjomataram I and Fidler- Benaoudia MM: Global patterns and trends in breast cancer incidence and mortality across 185 countries. Nat Med 31: 1154-1162, 2025.
2. Sung H, Ferlay J, Siegel RL, Laversanne M, Soerjomataram I, Jemal A and Bray F: Global cancer statistics 2020: GLOBOCAN estimates of incidence and mortality worldwide for 36 cancers in 185 countries. CA Cancer J Clin 71: 209-249, 2021.
3. Harbeck N, Penault-Llorca F, Cortes J, Gnant M, Houssami N, Poortmans P, Ruddy K, Tsang J and Cardoso F: Breast cancer. Nat Rev Dis Primers 5: 66, 2019.
4. Kannan K, Sivakumar S, Venkatesan T and Ali N: The underlying mechanisms and emerging strategies to overcome resistance in breast cancer. Cancers (Basel) 17: 2938, 2025.
5. Al Khzem AH, Gomaa MS, Alturki MS, Tawfeeq N, Sarafroz M, Alonaizi SM, Al Faran A, Alrumaihi LA, Alansari FA and Alghamdi AA: Drug repurposing for cancer treatment: A comprehensive review. Int J Mol Sci 25: 12441, 2024.
6. Seyyedabadi B, Babataheri S, Naseri M, Laher I and Soraya H: Ivermectin and non-parasitic disorders: An update. Curr Opin Pharmacol 85: 102574, 2025.
7. Kaur B, Blavo C and Parmar MS: Ivermectin: A multifaceted drug with a potential beyond anti-parasitic therapy. Cureus 16: e56025, 2024.
8. Hayashi A, Kamio K, Miyanaga A, Yoshida K, Noro R, Matsuda K, Tozuka T, Omori M, Hirao M, Fukuizumi A, *et al*: Ivermectin enhances paclitaxel efficacy by overcoming resistance through modulation of ABCB1 in non-small cell lung cancer. Anticancer Res 44: 5271-5282, 2024.
9. Zhang J, Zhang J, Feng Q, Jiang X, Yang Y, Liu W, Xiao J, Feng J, Wang Z, Pan M, *et al*: Purinergic receptor nanoimmunoamplifiers potentiate chemoimmunotherapy efficacy in hepatocellular carcinoma. Biomater Res 29: 0278, 2025.
10. Kuznetsov KO, Safina ER, Gaimakova DV, Frolova YS, Oganesyan IY, Sadertdinova AG, Nazmieva KA, Islamgulov AH, Karimova AR, Galimova AM and Rizvanova EV: Metformin and malignant neoplasms: A possible mechanism of antitumor action and prospects for use in practice. Probl Endokrinol (Mosk) 68: 45-55, 2022 (In Russian).
11. Song C, Jung D, Kendi AT, Rho JK, Kim EJ, Horn I, Curran GL, Ghattamaneni S, Shim JY, Kang PS, *et al*: Metformin prevents tumor cell growth and invasion of human hormone receptor-positive breast cancer (HR+ BC) Cells via FOXA1 inhibition. Int J Mol Sci 25: 7494, 2024.

12. Higurashi T and Nakajima A: Metformin and colorectal cancer. Front Endocrinol (Lausanne) 9: 622, 2018.
13. Basheer HA, Salman NM, Abdullah RM, Elsalem L and Afarinkia K: Metformin and glioma: Targeting metabolic dysregulation for enhanced therapeutic outcomes. Transl Oncol 53: 102323, 2025.
14. Li JH, Hsin PY, Hsiao YC, Chen BJ, Zhuang ZY, Lee CW, Lee WJ, Vo TTT, Tseng CF, Tseng SF and Lee IT: A narrative review: Repurposing metformin as a potential therapeutic agent for oral cancer. Cancers (Basel) 16: 3017, 2024.
15. Feng H, He L, Umar T, Wang X, Li W, Zhang B, Zhu X, Deng G and Qiu C: Synergistic antitumor effects of ivermectin and metformin in canine breast cancer via PI3K/AKT/mTOR pathway inhibition. Curr Issues Mol Biol 47: 403, 2025.
16. Mahfauz M, Yuruker O and Kalkan R: Repurposing metformin as a potential anticancer agent using in silico technique. Daru 32: 549-555, 2024.
17. Xia Y, Sun M, Huang H and Jin WL: Drug repurposing for cancer therapy. Signal Transduct Target Ther 9: 92, 2024.
18. Ayub A, Hasan MK, Mahmud Z, Hossain MS and Kabir Y: Dissecting the multifaceted roles of autophagy in cancer initiation, growth, and metastasis: From molecular mechanisms to therapeutic applications. Med Oncol 41: 183, 2024.
19. Li X, Liu S, Jin L, Ma Y and Liu T: NOD2 inhibits the proliferation of esophageal adenocarcinoma cells through autophagy. J Cancer Res Clin Oncol 149: 639-652, 2023.
20. Xu Z, Han X, Ou D, Liu T, Li Z, Jiang G, Liu J and Zhang J: Targeting PI3K/AKT/mTOR-mediated autophagy for tumor therapy. Appl Microbiol Biotechnol 104: 575-587, 2020.
21. Jiang ZM, Fang ZY, Yang X, Ji XX, Zhao YY, Lin BY, Weng ZB and Liu EH: Glycyrrhetinic acid ameliorates gastric mucosal injury by modulating gut microbiota and its metabolites via Thbs1/PI3K-Akt/p53 pathway. Phytomedicine 142: 156745, 2025.
22. Dong S, Liang S, Cheng Z, Zhang X, Luo L, Li L, Zhang W, Li S, Xu Q, Zhong M, *et al*: ROS/PI3K/Akt and Wnt/β-catenin signalings activate HIF-1α-induced metabolic reprogramming to impart 5-fluorouracil resistance in colorectal cancer. J Exp Clin Cancer Res 41: 15, 2022.
23. Tsai SC, Chang PC, Lin YT, Huang PT, Chen JY, Lin CS, Wu BN, Chang HM, Wu WJ, Chang CI and Lee CH: Repurposing of the antipsychotic trifluoperazine induces SLC7A11/GPX4-mediated ferroptosis of oral cancer via the ROS/autophagy pathway. Int J Biol Sci 20: 6090-6113, 2024.
24. Corbella E, Fara C, Covarelli F, Porreca V, Palmisano B, Mignogna G, Corsi A, Riminucci M, Maras B and Mancone C: THBS1 and THBS2 enhance the in vitro proliferation, adhesion, migration and invasion of intrahepatic cholangiocarcinoma cells. Int J Mol Sci 25: 1782, 2024.
25. Jiang M, Zhang K, Zhang Z, Zeng X, Huang Z, Qin P, Xie Z, Cai X, Ashrafizadeh M, Tian Y and Wei R: PI3K/AKT/mTOR axis in cancer: From pathogenesis to treatment. MedComm (2020) 6: e70295, 2025.
26. Bu X, Sha S, Zhang Z, Bian S, Feng S, Li C, Wang L and Chen H: Thrombospondin 1 aggravates cardiac remodeling in heart failure with preserved ejection fraction by inhibiting mitophagy. iScience 29: 114639, 2026.
27. Sayers EW, Beck J, Bolton EE, Brister JR, Chan J, Connor R, Feldgarden M, Fine AM, Funk K, Hoffman J, *et al*: Database resources of the National Center for Biotechnology Information in 2025. Nucleic Acids Res 53: D20-D29, 2025.
28. Liu A, Wang H, Lv H, Yang H, Li Y and Qian J: Autophagy inhibitor 3-methyladenine mitigates the severity of colitis in aged mice by inhibiting autophagy. Exp Gerontol 201: 112697, 2025.
29. Galicia-Moreno M, Monroy-Ramirez HC, Caloca-Camarena F, Arceo-Orozco S, Muriel P, Sandoval-Rodriguez A, García-Bañuelos J, García-González A, Navarro-Partida J and Armendariz-Borunda J: A new opportunity for N-acetylcysteine. An outline of its classic antioxidant effects and its pharmacological potential as an epigenetic modulator in liver diseases treatment. Naunyn Schmiedebergs Arch Pharmacol 398: 2365-2386, 2025.
30. Cabrera-Serrano AJ, Sánchez-Maldonado JM, González-Olmedo C, Carretero-Fernández M, Díaz-Beltrán L, Gutiérrez-Bautista JF, García-Verdejo FJ, Gálvez-Montosa F, López-López JA, García-Martín P, *et al*: Crosstalk between autophagy and oxidative stress in hematological malignancies: Mechanisms, implications, and therapeutic potential. Antioxidants (Basel) 14: 264, 2025.
31. Siavoshi A, Taghizadeh M, Dookhe E and Piran M: Gene expression profiles and pathway enrichment analysis to identification of differentially expressed gene and signaling pathways in epithelial ovarian cancer based on high-throughput RNA-seq data. Genomics 114: 161-170, 2022.
32. Jiang L, Fang T, Hu T, Feng J and Yan P: Mir-338-3p targeting THBS1 attenuates glioma progression by inhibiting the PI3K/Akt pathway. Biol Direct 19: 9, 2024.
33. Shen J, Zhou L, Ye K, Gong J, Wu F, Mo K, Zhu Y, Chen C and Zhan R: The role of SPI1/VSIG4/THBS1 on glioblastoma progression through modulation of the PI3K/AKT pathway. J Adv Res 71: 487-500, 2025.
34. Tuoheti K, Bai X, Yang L, Wang X, Cao Y, Yisha Z, Guo L, Zhan S, Wu Z and Liu T: Forsythiaside A suppresses renal fibrosis and partial epithelial-mesenchymal transition by targeting THBS1 through the PI3K/AKT signaling pathway. Int Immunopharmacol 129: 111650, 2024.
35. Zhou FL, Hu M, Hu J, Lin T and He YC: Maslinic acid induces autophagy through PI3K/Akt/mTOR pathway in human nasopharyngeal carcinoma cells. Chin Tradit Herb Drugs 51: 2481-2485, 2020.
36. Qin P, Li Q, Zu Q, Dong R and Qi Y: Natural products targeting autophagy and apoptosis in NSCLC: a novel therapeutic strategy. Front Oncol 14: 1379698, 2024.
37. Xin H and Xu W: Effect of licochalcone A on autophagy in renal cell carcinoma via PI3K/Akt/mTOR signaling pathway. Zhongguo Zhong Yao Za Zhi 43: 3545-3552, 2018 (In Chinese).
38. Yang H, Zhou J and Yang X: Effects of PicrosideII on autophagy of MCF-7 breast cancer cells and its mechanism. Chin J Clin Pharmacol Ther 24: 535-540, 2019.
39. Malekan M, Dozandeh-Jouybari A, Joudaki N, Ahangari M, Valadan R, Asgarian-Omran H and Taghiloo S: Inhibition of PI3K/AKT/mTOR signaling enhances autophagy in HL-60 acute myeloid leukemia cells: An integrative bioinformatic and in vitro study. Biochem Biophys Rep 44: 102220, 2025.
40. Liu Y, Cai X, Liu J, Luo Z, Zhang J, Cao Z, Ma W, Tang Y, Liu T, Wei H and Yu CY: The role of redox homeostasis in tumor progression: Implications for cancer therapy. Acta Biomater 204: 156-186, 2025.
41. Ma J, Wu Y, Huang D, Zhou Y, Hou L, Li Y, Zhong J and Wei X: Averrhoa carambola L. roots DMDD alleviates myocardial injury in diabetes mellitus mice by regulating ROS-mediated autophagy pathway. Chin Pharmacol Bull 37: 823-827, 2021.
42. Yu Y, Wang K, Zhu Y, Qi S and Luo L: Research progress on autophagy regulated tumor radiosensitivity[J]. Journal of Xuzhou Medical University 42: 771-775, 2022.